Mem. S.A.It. Vol. 93, 25

Memorie della

Seasonality of Viral Respiratory Diseases and Virucidal Power of Solar UV Photons

Fabrizio Nicastro[1] , Giorgia Sironi[2], Elio Antonello[2], Andrea Bianco[2], Mara Biasin[3], John R. Brucato[4], Ilaria Ermolli[1], Giovanni Pareschi[2], Marta Salvati[5], Paolo Tozzi[4], Daria Trabattoni[3], and Mario Clerici[6,7]

[1] Istituto Nazionale di Astrofisica – Osservatorio Astronomico di Roma, Via Frascati 33, I-00078 Monte Porzio Catone (RM), Italy e-mail: fabrizio.nicastro@inaf.it
[2] Istituto Nazionale di Astrofisica – Osservatorio Astronomico di Brera, I-20121 Milano, Italy
[3] University of Milano – Department of Biomedical and Clinical Sciences L. Sacco, I-20157 Milano, Italy
[4] Istituto Nazionale di Astrofisica – Osservatorio Astrofisico di Arcetri, I-50125 Firenze, Italy
[5] Regional Agency for Environmental Protection of Lombardia (ARPA Lombardia), I-20124 Milano, Italy
[6] University of Milano – Department of Pathophysiology and Transplantation, I-20157 Milano, Italy
[7] Don C. Gnocchi Foundation – IRCCS, I-20148 Milano, Italy

Received: 2 February 2022; Accepted: 25 February 2022

Abstract. Seasonality of acute viral respiratory diseases is a well-known and yet not fully understood phenomenon. The course of the SARS-Cov-2 pandemics has showed no exception. In this contribution, we show that: (a) the seasonality of viral respiratory diseases, as well as its distribution with latitude on Earth, can be fully explained by the virucidal properties of UV-B and A Solar photons through a daily, minute-scale, resonant forcing mechanism; (b) UV-B/A photons have a powerful virucidal effect on the single-stranded RNA virus Covid-19 and the Solar radiation that reaches temperate regions of the Earth at noon during summers, is sufficient to inactivate 63% of virions in open-space concentrations in less than 2 minutes.

Key words. Epidemiology: seasonality – Virology: SARS-CoV-2, UV virucidal power – Solar Physics: UV-B-A on Earth

1. Introduction

Several models have been proposed to explain the regularity of yearly recurring outbreaks of acute respiratory diseases, and their phase-differences at different latitudes on Earth (e.g. Lofgren et al., 2007 and references therein). Internal biological dynamics that allow influenza viruses to evade host's immunity and become more virulent (Cox and Subbarao, 1999), manifest mainly through "antigenic drift", the property of such viruses to mutate rapidly (Agranovski et al., 2004; 2005). For A and B influenza viruses, such mutations develop at rates of about 12 and 6 mutations per RNA segment per year (Logfren et al., 2007; McCullers et al., 1999), about 2-4 times the

mutation rate estimated for the Covid-19 virus (e.g. Morales et al., 2021). These rates are sufficient (especially for type-A influenza) to trigger recurrences of epidemics on antigenic-drift timescale. However, without an external forcing mechanism, such recurring events are typically of modest intensity, can only last for a few cycles, and most importantly are not able to reproduce the observed phase-shift between north and south hemisphere on Earth.

One or more concurring external mechanisms must be invoked to explain all evidence, and several have been proposed: weather-related temperature and humidity oscillations on Earth (e.g. Baker et al., 2020), the observed yearly pattern of air-travel (e.g. Grais et al., 2003, but see also Grais et al., 2004), indoor heating during winter (e.g. Liao et al., 2005), bulk aerosol transport of virus through global convective currents or related to weather oscillations like "El Niño" (e.g. Ebi et al., 2001; Viboud et al., 2004). Most of these, however, can only explain, singularly, some aspects of seasonality of recurring outbreaks, or the onsets of particularly violent outbreaks. For example, the load of air-travel flow is typically larger during northern hemisphere summers, and this is in contrast with most of the outbreaks developing during falls and winters in these countries. On the other hand, vastly populated areas in the north hemisphere lie at relatively low latitudes in temperate regions where indoor heating is not massively widespread: yet, even in these areas, influenza epidemics typically develop during winters, and remain inactive in summers. Similarly, temperature, humidity, as well as air pollution, are not homogeneously distributed through the planet, and micro-climate can vary substantially at the same latitude, depending on the particular geographical or industrial setting of even contiguous areas. The cross-influence of all these factors could certainly synergize to produce the observed geographical and time modulations, but this would require a hard to obtain perfect fine-tuning of the many parameters at play.

The one mechanism that has been acting constantly at (almost) the same pace every day of the year and every year for the past four billion years, is the irradiation of the Sun on Earth. At a given location on Earth, this is modulated daily by the Earth's spinning and yearly by the Earth's orbit around the sun. Solar ultraviolet photons with wavelength in the range 200-290 nm (UV-C radiation) photo-chemically interact with DNA and RNA and are endowed with germicidal properties that are also effective on viruses (Kowalski, 2009; Rauth, 1965; Kesavan and Sagripanti, 2012; Chang et al., 1985; McDevitt et al., 2012; Welch et al., 2018; Walker and Ko, 2007; Tseng and Li, 2005). Fortunately, UV-C photons are filtered out by the Ozone layer of the upper Atmosphere, at around 35 km (e.g. Walker and Ko, 2007). Softer UV photons from the Sun with wavelengths in the range 290-320 nm (UV-B) and 320-400 nm (UV-A), however, do reach the Earth's surface. The effect of these photons on Single- and Double-Stranded RNA and DNA viruses (e.g. Lytle and Sagripanti, 2005; Lubin and Jense, 1995) and the possible role they play on the seasonality of epidemics e.g Martinez, 2018), are nevertheless little studied.

Here we first briefly introduce our mathematical model of epidemics that includes the effect of Solar UV photons ("solar-pump", hereinafter: Nicastro et al., 2020) and show that is able to naturally reproduce the seasonality of influenza-like epidemics without forcing seasonal oscillations with ad-hoc mathematical prescriptions (e.g. Dushoff et al., 2004; Neher et al., 2020). We then combine (*i*) our measurements of the action spectrum of Covid-19 in response to UV light (Biasin et al., 2022) , (*ii*) Solar irradiation measurements on Earth during the SARS-CoV-2 pandemics (from the Tropospheric Emission Monitoring Internet Service (TEMIS) archive: `http://www.temis.nl`), (*iii*) worldwide recorded Covid-19 mortality data (from the GitHub repository provided by the Coronavirus Resource Center of the John Hopkins University - JHU-CRC: `https://github.com/CSSEGISandData/COVID-19`) and (*iv*) our "Solar-Pump" diffusive model of epidemics, to show that the Solar radiation that reaches temperate regions of the Earth at noon during summers, is sufficient to inactivate 63% of virions in open-space concentrations

(precisely, 1.5×10^3 Median Tissue Culture Infectious Dose per ml - $TCID_{50}$/ml - concentrations, i.e. higher than typical aerosol) in less than 2 minutes. We conclude that the characteristic seasonality imprint displayed world-wide by the SARS-Cov-2 mortality time-series throughout the diffusion of the outbreak (with temperate regions showing clear seasonal trends and equatorial regions suffering, on average, a systematically lower mortality), might have been efficiently set by the different intensity of UV-B/A Solar radiation hitting different Earth's locations at different times of the year. Our results suggest that Solar UV-B/A play an important role in planning strategies of confinement of epidemics, which should be worked out and set up during spring/summer months and fully implemented during low-solar-irradiation periods.

2. The Solar-Pump Model

Our SIR-like (Susceptible–Infected-Recovered/Deaths) "Solar-Pump" model is discussed in details in Nicastro et al. (2020). Here, we briefly summarize the main ingredients of the model. The model considers isolated (i.e. no cross-mixing), zero-growth (i.e. death rate equal to birth rate), groups of individuals in whom an efficacious anti-viral immune response has either been elicited ($Susceptible \rightarrow Infected \rightarrow Recovered$: SIR) or not ($Susceptible \rightarrow Infected \rightarrow Recovered \rightarrow Susceptible$: SIRS). The inefficiency of the natural (disease) and induced (vaccines) anti-viral immune response is parameterized through population loss-of-immunity (LOI) rates.

For a given set of initial and/or boundary conditions, unique solutions of the model are obtained by integrating, the following set of 1^{st}-order differential equations, in which the $Susceptible$ population (S) interacts not linearly with $Infected$ (I) at a rate β (proportional to the reproductive parameter R_t: with $R_{t=0} = R0$ being the intrinsic reproductive number of the epidemic), recovers (R) or dies (D) with rates γ_{out} and μ, respectively, get vaccinated (V) at a rate ξ_{out}, and can become again susceptible with loss-of-immunity (LOI) rates γ_{in} (natural) and ξ_{in} (vaccines):

$$\begin{aligned}
\frac{dS}{dt} &= -\beta\frac{SI}{N} - \xi_{out}S + \gamma_{in}R + \xi_{in}V \\
\frac{dI}{dt} &= \beta\frac{SI}{N} - (\gamma_{out} + \mu)I \\
\frac{dR}{dt} &= \gamma_{out}I - \gamma_{in}R \\
\frac{dD}{dt} &= \mu I \\
\frac{dV}{dt} &= \xi_{out}S - \xi_{in}V
\end{aligned} \tag{1}$$

The Solar virus inactivation mechanism (Solar-Pump) is introduced by modulating the rate of contacts β between susceptible and infected individuals through the factor $(1–\epsilon sin(\theta))$, where θ is the solar elevation angle (function of Earth's latitude α, time of the day h and day of the year t) and ϵ is the efficiency of the mechanism. The efficiency ϵ is evaluated at noon at a given Earth's latitude α and day of the year t, based on our laboratory data on the covid-19 virus (see below, and Nicastro et al., 2021, for a full treatment). Model solutions have a time resolution of 1 day and infra-day modulations of the solar–pump efficiency are obtained by integrating daily to a sub-resolution of ~ 1.5 minutes.

Figure 1 shows typical yearly (main panel) and infra-day (onsets) R_t modulations of an intrinsic reproduction number $R0 = 3$, imprinted by the solar mechanism (see details in Figure's caption).

Figure 2 shows, as an example, our model predictions for the first 20 years of annual Influenza outbreaks at three different latitudes on Earth, +40 degrees north (black), -40 degrees south (blue) and the Equator (orange), with (panel (a)) and without ($\epsilon = 0$; panel (c)) active solar-pump. When the solar-pump is active (panels (a) and (b)) constructive resonance builds-in regular sun-modulated oscillations already after the first 2 cycles, and the strength of the seasonal outbreaks adjust to constant values that depend on latitude. Without solar-pump (panels (c) and (d)) the cycles follow the LOI period and are the same at all latitudes: the epidemics quickly die out in a

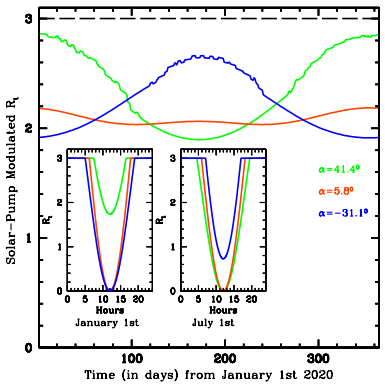

Fig. 1. Main panel: day-by-day yearly modulation imprinted by the solar mechanism on the intrinsic reproduction number $R0 = 3$ of the epidemic (black horizontal dashed line), at three average latitudes on Earth, corresponding to the North (green curves), South (blue curves) and Tropical (orange curves) inhabitated areas, as labeled. Onsets: infra-day solar-pump modulation of $R0$ at the three latitudes on January 1st (left onset) and July 1st (right onset) 2020, as labeled.

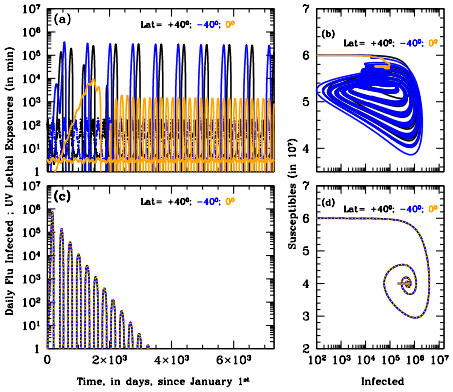

Fig. 2. Panels (a) and (c): curves of growths of the daily new infected for the first 20 years of annual Influenza outbreaks at three different latitudes on Earth, as labeled, with (panel (a)) and without ($\epsilon = 0$; panel (c)) active solar-pump. Model parameters are t_0 = January 1st, $t_{end} = t_0 + 100$ years, $R0 = 1.5$, $\gamma_{out} = 0.2$, $\gamma_{in} = 0.0055$, $\mu = 0.001$ and no external lockdown or phase-2. Yearly oscillating dotted curves at the bottom of the top panel are UV-B/A lethal-exposure for an arbitrary efficiency and are reported here only to mark winter peaks and summer minima. Panels (b) and (d): S–I phase diagrams for the simulations of panels (a) and (c), respectively. The first 100 years of the epidemics are plotted (every other 10 years, in panel (b), for easier visualization.

few years, because of lack of supply among the susceptible population.

3. Effects of Solar UV Photons on the SARS-CoV-2 Pandemics

To evaluate the potential of Solar UV-B/A photons on the onset, diffusion and strength of the recent SARS-CoV-2 pandemics, in our analysis we use the Covid-19 action spectrum (i.e. the ratio of the virucidal dose of UV radiation at a given wavelength to the lethal dose at 254 nm) recently compiled by us in the laboratories of the University of Milan (Biasin et al., 2022; see Fig. 1 in Nicastro et al., 2021), together with UV-B and –A solar radiation measurement estimates on the Earth as a function of Earth's latitude and day of the year (Zempila et al., 2001). The action spectrum of Covid-19 in response to D_{63} UV doses (the amount of UV photons needed to inactivate 63% of the virions) is at least 2 orders of magnitude more efficient than that of direct DNA-damage (`https://www.temis.nl/uvradiation/product/action.html`) or that obtained by extrapolating to longer wavelengths the action spectrum of Lytle & Sagripanti (2005), derived for a compilation

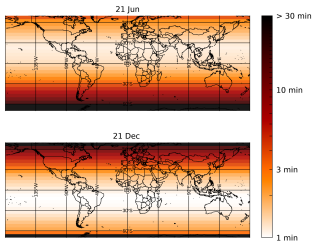

Fig. 3. Two world maps with a superimposed Covid-19, monthly-averaged, lethal-times (τ_{63}) intensity-gradient image, at summer (top panel) and winter (bottom panel) solstices.

of a wide variety of viruses (see, e.g. Fig. 1 in Nicastro et al., 2021 and Fig. 6 in Biasin et al., 2022). As a consequence, "instantaneous" Solar lethal-times τ_{63}, i.e. the time needed for the Sun to deliver a lethal dose D_{63} at a given time of the day and location on the Earth, are relatively short (Fig. 3). Less than 2 minutes are needed at noon, all year round, to inactivate 63% of Covid-19 in aerosol or on surfaces in equatorial regions (Figure 3). This is also the case for temperate-region locations ($20 < |\alpha| < 60$ degrees) during boreal (Fig. 3, upper panel) and austral (Fig. 3, lower panel) summers, but then lethal times in these regions start increasing steadily by up to factors of 20 from falls through winters, to then decrease again in Spring.

To investigate the effect of this radiation on the diffusion and strength of the SARS-CoV-2 pandemics, we collected Covid-19 data from the JHU-CRC archive. Figure 4 shows that the absolute maximum number of daily SARS-CoV-2 deaths per million inhabitants (mortality) reached in each Country of our sample, anti-correlates with the Solar-UV inactivation index Ξ on the Earth 3 weeks prior to the mortality peak (see Figure's caption for details). We did not attempt to correct the data for social-distancing measures (adopted differently and at different times of the years in different regions of the world) or for tropical daily cloud-coverage (where present systematically, like in equatorial Countries during rain versus dry seasons), or to normalize by the fraction of elderly population in each Country (information not provided with the JHU-CRC data). All these factors certainly contribute significantly to the scatter visible in the data (main plot) and, indeed, greatly reduced when these are grouped in either latitude or Solar Inactivation Index bins (left and right onsets, respectively). Nonetheless, the correlation in Fig. 3 is statistically highly significant and extends more than one order of magnitude in Ξ and over four orders of magnitude in mortality. Simple linear-regression tests of the data-points (Pearson) and their rankings (Spearman), yield null (i.e. chance correlation) probabilities of $p = 6.4 \times 10^{-12}$ and $p = 2.0 \times 10^{-12}$, respectively, corresponding to Gaussian-equivalent significances of 6.8σ and 7σ.

4. Discussion and Conclusions

The high efficiency of Solar UV inactivation power against Covid-19, had already been suggested by previous works, based on either general models on coronaviruses (e.g. Sagripanti & Lytle, 2020), observed anti-correlation between sunlight doses and SARS-CoV-2 positive cases (e.g. Tang et al., 2021]) and/or actual experiments with simulated sunlight (e.g. Ratnesar-Shumate et al., 2020). Particularly, the comparison between predictions (Sagripanti & Lytle, 2020) and actual measurements of Covid-19 exposure to artificial Solar radiation (Ratnesar-Shumate et al., 2020), suggested the importance of UV-A photons (Luzzatto-Fegiz et al., 2020, 2021). Ratnesar-Schumate and collaborators (2020) found that 6.8 minute of continuous exposure of dried saliva-like concentrations of Covid-19 to simulated sunlight in summer at a latitude of 40 degrees were sufficient to inactivate 90% of virions. Our experiments use almost monochromatic UV light on even higher, but non-dried, concentrations (1.5×10^3 $TCID_{50}$/ml) of Covid-19 and find 90% lethal times in summer at similar latitudes a factor of about 2 shorter. This difference could be at least partly due to the difficulty in properly subtracting the effect of the additional optical

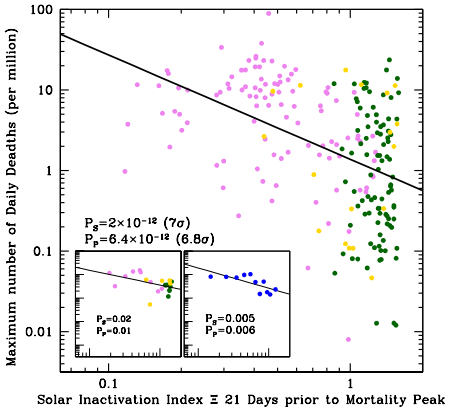

Fig. 4. Absolute maximum number of daily SARS-CoV-2 deaths per million inhabitants, as recorded over the period 22 January 2020 - 2 May 2021 for the 214 Countries (or territories) of our sample, versus the Solar UV Inactivation index Ξ on the Earth 3 weeks prior to the mortality peak. The Solar UV Inactivation Index Ξ is defined as the ratio of the Solar UV power administered in 2 minute to the Covid-19 lethal dose D_{63}. Pink, green and yellow circles are Countries of the north hemisphere ($\alpha > 20$ degrees: 103 Countries), the equatorial strip ($|\alpha \leq 20$ degrees: 93 Countries), and the south hemisphere ($\alpha < -20$ degrees: 18 Countries). Grouping the data in either 5-degree-wide latitude bins (left onset) or 0.1-wide Ξ bins (right onset) greatly reduces the scatter present in the main plot, but also the degrees of freedom of the relations, thus yielding to higher (but still low) probabilities of chance correlation.

depth introduced by the process of desiccation of the samples prior to sunlight exposure (e.g. Sagripanti & Lytle, 2011), which might have artificially increased the exposure needed to inactivate the virions in the experiment by Ratnesar-Shumate and collaborators (2020).

Seasonal air temperature oscillations on temperate regions of the Earth, as well as large day/night thermal excursion in dry and low-latitude regions, are due to the different amount of Solar radiation hitting different locations on the Earth's surface at different times of the year. The two quantities are therefore obviously broadly correlated. However, at Earth's temperature heat itself cannot be the direct cause of virus inactivation in summers or at the equator in open-spaces, since Covid-19 is known to survive to non-Earth-like temperatures of 60-70 ^{0}C, for up to 10 minutes and to continuous exposure to extreme, but more common, summer-like temperatures of 37 ^{0}C for longer than 6 hours (Chin et al., 2020). However, heat (i.e. high air temperatures), in low-humidity environments, can certainly boost the direct disinfecting power of Solar UV-B/A radiation, by speeding up the evaporation of water droplets containing virions (e.g. Dbouk & Drikakis, 2020). Humidity, instead, is likely to play against Solar UV-B/A inactivation power, by both hampering efficient water droplet evaporation and by increasing the optical depth to disinfecting radiation. This has indeed been observed (e.g. Li, Wang & Nair, 2020; Baker, Yang & Vecchi, 2020), particularly in equatorial regions where a year-round risk of coronavirus infection is present (Li, Wang & Nair, 2020), albeit with consistently lower mortality (green points in Fig. 3), due probably to the combined effect of the high and almost constant amount of UV-B/A radiation administered by the Sun over time, and the increased optical depth due to high humidity .

Our results shows that Solar UV-A/B are highly efficient in inactivating SASR-Cov-2: less than 2 minutes are needed at noon, all year round, to inactivate 63% of Covid-19 in aerosol or surfaces in equatorial regions, and during temperate-location summers. We also show that such high-efficiency virucidal mechanism had probably a role in modulating the strength and diffusion of the SARS-CoV-2 epidemics, explaining the geographical and seasonal differences that characterize this disease. They also imply, if confirmed, that the UV flux received from our Sun in open areas may represent an important disinfection factor, able to significantly reduce the diffusion of the pandemics.

Acknowledgements. The work presented in this paper has been carried out in the context of the activities promoted by the Italian Government and in particular, by the Ministries of Health and of University and Research, against the COVID19 pandemic. Authors are grateful to former and cur-

rent INAF's Presidents, Prof. N. D'Amico and M. Tavani, for strongly supporting this initiative.

References

Agranovski, I. E., et al., 2005, J. Aerosol Sci, 36, 609–617

Agranovski, I. E., et al., 2004, Appl. Environ. Microbiol, 70, 6963–6967

Baker R. E., Yang W. and Vecchi G. A., 2020, Science, 10, 1126–1129

Biasin, M. et al., 2022, Journal of Photochemistry and Photobiology, 10, 100107

Chang J.C. et al., 1985, Appl. Env. Microb., 49: 1361-1365

Chin A.W.H. et al., 2020, The Lancet Microbe, 1(1), E10

Cox, N. J., and K. Subbarao, 1999, The Lancet, 354,1277–1282

Dbouk T. and Drikakis D., 2020, Physics of Fluids, 32, 093312

Dushoff J. et al., 2004, PNAS, 101, 48, 16915–16916

Ebi, K. L. et al., 2001, Am. J. Public Health, 91,1200–1208

Grais, R. F. et al., 2004, Science, 7, 127–134

Grais, R. F., J. H. Ellis and G. E. Glass, 2003, J. Epidemiol, 18, 1065–1072.37

Kesavan, J.S. and Sagripanti, J.L., 2014, in Aerosol Science (eds I. Colbeck and M. Lazaridis), doi:10.1002/9781118682555.ch17

Kowalski W., 2009, Eds. Springer-Verlag, doi: 10.1007/978-3-642-01999-9

Li Y., Wang X. and Nair H., 2020, Journal of Infectious Diseases, doi: 10.1093/infdis/jiaa436

Liao, C. M., C. F. Chang and H. M. Liang, 2005, Risk. Anal., 25,1097–1107

Lofgren E., Fefferman N. H., Naumov Y.N., Gorski J., and Naumova E.N., 2007, Journal of Virology, 81, 5429–5436

Lubin D. and Jensen E.H., 1995, Nature, 377, 710–713

Luzzatto-Fegiz P. et al., 2021, The Journal of Infectious Diseases, 223, Issue 8, 1500–1502

Luzzatto-Fegiz P. et al., 2021, bioRxiv preprint, doi:10.1101/2020.09.07.286666

Lytle D.C. and Sagripanti J.L., 2005, J. Virol., 79, 14244–14252

McCullers, J. A. et al., 1999, J. Virol, 73, 7343–7348

McDevitt J.J., Rudnick S.N. and Radonovich L., 2012, Appl Environ Microbiol, 78, 1666–1669

Martinez M.E., 2018, PLoS Pathog, 14(11): e1007327, doi: https://doi.org/10.1371/journal.ppat.1007327

Morales-Castillo, A. et al., 2021, Genome Biology and Evolution, 13, 10

Neher R.A. et al., 2020, Swiss Med Wkly, 150, w20224

Nicastro, F. et al., 2020, iScience, vol. 23, issue 10, p. 101605

Nicastro, F. et al., 2021, Scientific Reports, 11, 14805

Ratnesar-Shumate S. et al. 2020, The Journal of Infectious Diseases, 222, 214–222

Rauth AM, 1965, Light Biophys J, 5: 257–273

Sagripanti J.L. and Lytle D.C., 2020, Photochemistry and Photobiology 96 (4), 731–737

Sagripanti J.L. and Lytle D.C., 2011, Arch. Virol., 156, 489–494

Tseng C.C. and Li C.S., 2005, Aerosol Science and Technology, 39, 1136-1142

Viboud, C., K. et al., 2004, Eur. J. Epidemiol, 19, 1055–1059

Walker C.M. and Ko G., 2007, Environ Sci Technol, 41, 5460-5465

Welch, D.et al., 2018, Scientific Reports, 8, 2752